

Exergy analysis of a diesel engine with Waste Cooking Biodiesel and Triacetin

Chukwuka Odibi⁽¹⁾, Meisam Babaie⁽¹⁾, Ali Zare⁽²⁾, Md. Nurun Nabi⁽³⁾, Timothy A. Bodisco⁽²⁾, Richard J. Brown⁽⁴⁾

⁽¹⁾ *School of Science, Engineering and Environment, University of Salford, Salford, Manchester M5 4WT, United Kingdom*

⁽²⁾ *Flow, Aerosol & Thermal Energy (FATE) Group, School of Engineering, Deakin University, VIC 3216, Australia*

⁽³⁾ *Central Queensland University, Perth, WA 6000, Australia*

⁽⁴⁾ *Biofuel Engine Research Facility (BERF), Queensland University of Technology (QUT), QLD 4000, Australia*

Abstract

This study uses the first and second laws of thermodynamics to investigate the effect of oxygenated fuels on the quality and quantity of energy in a turbo-charged, common-rail six-cylinder diesel engine. This work was performed using a range of fuel oxygen content based on diesel, waste cooking biodiesel, and a triacetin. The experimental engine performance and emission data was collected at 12 engine operating modes. Energy and exergy parameters were calculated, and results showed that the use of oxygenated fuels can improve the thermal efficiency leading to lower exhaust energy loss. Waste cooking biodiesel (B100) exhibited the lowest exhaust loss fraction and highest thermal efficiency (up to 6% higher than diesel). Considering the exergy analysis, lower exhaust temperatures obtained with oxygenated fuels resulted in lower exhaust exergy loss (down to 80%) and higher exergetic efficiency (up to 10%). Since the investigated fuels were oxygenated, this study used the oxygen ratio (OR) instead of the equivalence ratio to provide a better understanding of the concept. The OR has increased with decreasing engine load and increasing engine speed. Increasing the OR

30 decreased the fuel exergy, exhaust exergy and destruction efficiency. With the use of B100,
31 there was a very high exergy destruction (up to 55%), which was seen to decrease with the
32 addition of triacetin (down to 29%).

33 **Keywords:** Energy analysis; exergy analysis; waste cooking biodiesel; fuel oxygen content;
34 exergetic efficiency.

35

36 1. INTRODUCTION

37 The world's energy demand, which is driven by population and economic growth, is
38 continuously increasing, with a 48% energy growth projection between 2012 and 2040, while
39 fossil fuel has been forecast to meet approximately three-quarters of the total energy demand
40 in 2040 [1]. This growth is potentially problematic, owing to diminishing non-renewable
41 reserves, large-scale environmental degradation in the form of global warming, and
42 atmospheric pollution due to the products of combustion of these fuels. To overcome the
43 challenges posed by fossil fuel, renewable and alternative energy sources are being sought now,
44 more than ever.

45 Biodiesel offers many advantages as an alternative fuel because it is renewable, energy efficient,
46 sulphur free and biodegradable [2, 3]. This alternative energy source can satisfy strict emission
47 rules in some applications and can potentially be used in existing diesel engines. However, it
48 performs differently and has different combustion characteristics compared to diesel fuel, and
49 thus, requires analysis from different points of view to fully appraise its utility as an alternative.

50 The chemical and physical properties of the biofuels such as the biodiesel chain are the key
51 parameters on engine performance and emissions [4, 5].

52 The effect of these fuels on engine performance has been mainly considered using the first law
53 of thermodynamics (energy analysis), as it quantitatively evaluates the energy in the process
54 [6]. However, further clarification with the use of the second law of thermodynamics (exergy
55 analysis) can be achieved for the system inefficiencies. Exergy analysis involves the
56 application of exergy concepts, balances and efficiencies to evaluate and improve the system
57 performance. It qualitatively and quantitatively determines losses in a system and locations
58 where they occur as sources of irreversibilities, and provides more accurate information about
59 engine efficiencies [7, 8]. This has rekindled interest in the second law of thermodynamics
60 (exergy analysis), as the use of the first law of thermodynamics (energy analysis) only to
61 evaluate engine performance has the limitation of not being able to evaluate some features of
62 energy degradation [9, 10].

63 With the rationale of better understanding the performance and sensitivity of various operating
64 parameters of internal combustion engines when operating with biodiesel, some studies have
65 considered the use of energy and exergy analysis to evaluate engine performance [11-13].
66 Karthikeyan et al. [14] compared three blends of rice bran biodiesel with pure diesel using
67 energy and exergy analysis. As reported by Cavalcanti et al. [12], engine at higher load with
68 biodiesel blends operates with higher exergetic efficiency. Rakopoulos and Giakoumis [15]
69 used computer analysis to study the energy and exergy performance of a diesel engine
70 operating under transient engine operating conditions, and they revealed how exergy properties
71 vary with different operating parameters. The first and second law analysis of a four-cylinder
72 direct injected diesel engine fuelled with diesel and peanut oil biodiesel blend were considered
73 in another study [16]. Using a Fortran-based code, Jafarmadar and Nematy [17] studied the
74 performance of diesel/biodiesel blends in a homogenous charge compression ignition engine
75 using a three-dimensional model. The exergy analysis showed the improvement of exergy
76 efficiency with an increase in volume percentage of biodiesel. Meisami and Ajam [18]

77 performed both energy and exergy analysis on a diesel engine using castor oil biodiesel with a
78 190 kW SHENCK engine dyno when operated at full load. From the result of their analysis,
79 the brake thermal efficiency and exergetic efficiency of the 15% castor oil blend was seen to
80 equal the diesel fuel (0% blend) with low exhaust gas efficiency. A single-cylinder, water-
81 cooled diesel engine was tested by Sayin Kul et al. [19] with varying quantities of biodiesel-
82 diesel blends containing 5% bioethanol operated at different speeds. It was seen that the pure
83 diesel fuel had slightly higher thermal and exergetic efficiencies when compared to the
84 biodiesel blend. However, a study by Zare et al. [20] with the engine used in current research
85 showed that using 100% waste cooking biodiesel increases the thermal efficiency by up to 5%
86 for the engine used in this study.

87 Fuel oxygen content has been introduced as an influential factor in engine performance and
88 emissions [20-25]. Song et al. [23] investigated the effect of oxygen content on combustion in
89 single- and multi-cylinder diesel engines using rapeseed biodiesel to vary the oxygen content
90 of the diesel used. From the results obtained, using oxygenated fuel was associated with a
91 subsequent increase in NO_x emissions. Effect of the fuel oxygen content on hydrocarbon
92 formation in diesel engine has been studied recently [26]. It was found that in oxygen-rich
93 condition, combustion temperature was the main influencer on the hydrocarbon formation. Jena
94 and Misra [24] used two different biodiesels separately - palm and karanja. The biodiesels had
95 differing oxygen content and they compared the energetic and exergetic efficiencies in a
96 compression ignition engine. The palm biodiesel, which had higher oxygen content, gave a
97 higher thermal efficiency with less associated irreversibility. Given the thermal efficiency as
98 the ratio of the output power to the input energy from the fuel, with the same output power
99 during the test, lower calorific value of the palm biodiesel was reported to be the reason for the
100 higher thermal efficiency of palm biodiesel. It also concluded that better combustion with less
101 irreversibility was possible with a further increase in the oxygen content of the fuel. This is

102 seen in a further study by Zare et al. [20], considering the performance and emissions of waste
103 cooking biodiesel blends whose oxygen content was increased with the addition of triacetin. In
104 previous studies with the same engine and fuels, engine performance and emissions (such as
105 NO_x and PM) has been reported during modal cycles [22], steady-state and transient operation
106 [21, 29] and cold start operation [30]. Compared to diesel with no oxygen content, when it
107 comes to alternative fuels in the market, fuel oxygen content will be an important fuel
108 properties which significantly affects the engine performance and emissions. With a reduction
109 in most exhaust emissions and little insight to the exergy analysis in previous studies conducted
110 by this research group, an exergy-based performance analysis can provide insight to the losses
111 associated with the system [27, 28]. As a result, a detailed evaluation of fuel efficiency as well
112 as irreversibility can be developed.

113 To the knowledge of authors, the effect of fuel oxygen content on exergetic parameters of diesel
114 engine performance in such a wide range has not been studied in the past. In this study, the first
115 and second laws of thermodynamics are used to analyse the quantity and quality of energy
116 produced by diesel and biodiesel blends operated at three different engine speeds and four
117 different loads. The experiments aimed to study the increase in the oxygen content of the blends
118 with the use of triacetin, which has a high oxygen content. Performance parameters were
119 analysed, including the power produced by the engine, brake specific fuel consumption (BSFC),
120 brake thermal efficiency (BTE), fuel energy and exergy, exergetic efficiency, exergy
121 destruction heat and exhaust losses, as well as other irreversibilities associated with operating
122 the engine at different loads and speeds, and with different biodiesel blends. These performance
123 parameters were graphically represented to establish the relationships between the
124 aforementioned variables.

125 As the aim of this manuscript is to study the effect of oxygen content on exergy-related
126 parameters, there is no intention to introduce a new fuel/mixture in this study. However, this

127 aspect has been analysed on European Stationary Cycle (ESC) and non-road transient cycle
128 (NRTC) in this research group [21, 22] to evaluate the possibility of using such fuels for Euro
129 III engines.

130

131 **2. MATERIALS AND METHODS**

132 2.1 Engine specification, experimental setup and design of experiment

133 The engine used for this experimental study was a turbo-charged, common-rail, six-cylinder
134 after-cooled diesel engine whose specification is shown in Table 1. The engine load was
135 controlled using an electronically controlled water-brake dynamometer which was coupled
136 with this engine.

137 Table 1. Specification of experimental engine setup

Model	Cummins ISBe220 31
Emission standard	Euro III
Cylinders	6 in-line
Aspiration	Turbocharged
Capacity	5.9L
Compression ratio	17:3:1
Bore x Stroke	102 x120 (mm)
Maximum torque	820 Nm @ 1500 rpm
Maximum Power	162 kW 2500 rpm
Dynamometer type	Hydraulic
Fuel injection	High pressure common rail

138

139 The schematic diagram for the experimental setup is presented in Fig. 1. A small fraction of
140 diesel exhaust was passed through a HEPA filter and then gas analysers to measure the gaseous
141 emissions. For CO₂ and NO_x measurement, CAI-600 CO₂ and CAI-600 CLD NO/NO_x were
142 used in this study. A Testo 350 XL Portable Emissions Analyser was also used to measure HC
143 and CO. The exhaust was passed through a dilution tunnel before measuring the particle
144 emissions. PM measurement was done with DustTrak II Aerosol Monitor 8530 (TSI) While a

145 SABLE CA-10 was used to measure CO₂ for calculating the dilution ratio. Table 2 shows the
146 accuracy of the measurement systems used for this study.

147

148

149

150

151

152

153

154

155

156

157

158

159

160

161

162

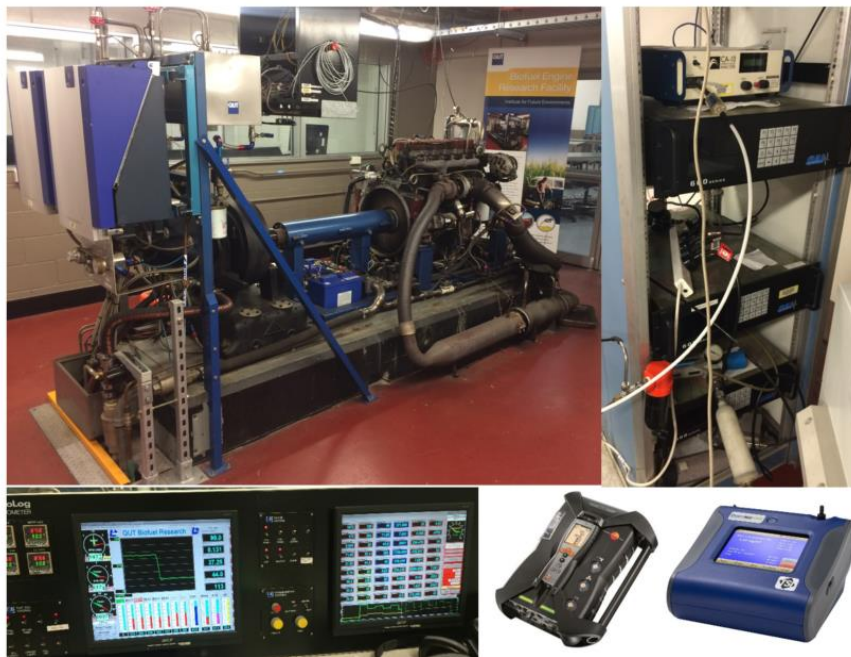
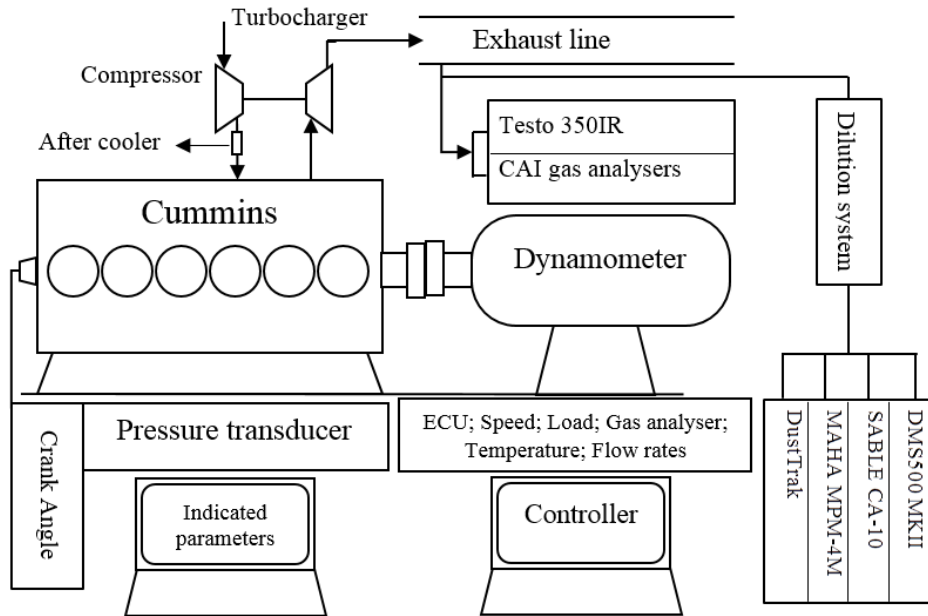
163

164 Table 2. The accuracy of instruments

Measurement instruments	Types of exhaust gases	Range	Accuracy	Flow rate (L min-1)
CAI-600 CLD NO/NOx Chemiluminescence (CLD) Photodiode (thermally stabilized with Peltier Cooler)	NO/NOx	0-1 to 3,000 ppm	RESPONSE TIME: T90 < 2 Seconds to 60 Seconds Adjustable RESOLUTION=10 ppb NO/NOX (Displays 5 significant digits) REPEATABILITY > 0.5% of Full Scale LINEARITY > 0.5% of Full Scale NOISE < 1% of Full Scale	0.3-3.0
CAI-600 CO2 Non-Dispersive Infrared (NDIR)	CO2	0-1000/2000/3000 ppm	RESPONSE TIME (IR): T90 < 2 Seconds to 60 Seconds Adjustable (Depending on configuration) RESOLUTION Displays Five Significant Digits REPEATABILITY > 1.0% of Full Scale LINEARITY > 0.5% of Full Scale NOISE < 1% of Full Scale	0.25 to 2.0
Sable CA-10 CO2 Analyser	CO2	0 – 5% standard 0 – 10% optional	1% of reading	5-500(x 10-3)
Testo 350 XL Portable Emission Analyser	SO2 CO CO2 O2 NO NO2 HC	0 – 5000 ppm 0 – 10,000 ppm 0 – CO2 max 0 – 25% 0 – 3000 ppm 0 – 500 ppm 0 – 60,000 ppm	5% of mv 5% of mv - 0.8% of fv 5% of mv 5 ppm 60 ppm	1.2
DustTrakTM II Aerosol Monitor 8530 (TSI)	PM1 PM2.5 PM10	0.001 – 400 mg m-3	5%	3.0

165

166



167 Fig. 1. Experimental setup

168

169 Since the engine used in this study was a Euro III engine, the operating modes were selected
 170 from the European Stationary Cycle (ESC) schedule. This cycle is a legislated test cycle for
 171 heavy-duty engines in the Euro III jurisdiction. In this experiment, 12 engine operating modes

172 from the ESC comprising three engine speeds (1472, 1865 and 2257 rpm) and four engine
173 loads (25, 50, 75 and 100 %) were used.

174

175 2.2 Fuel properties

176 Diesel (D100), waste cooking biodiesel (B100), and varying proportions of both/either diesel
177 and/or waste cooking biodiesel served as the primary fuel, with triacetin (T). Triacetin was
178 added to waste cooking biodiesel in order to study a wide range of fuel oxygen content. A total
179 of six different fuels were used in this experiment and are denoted by the portion of each fuel
180 in the final fuel, as displayed in the first row of Table 3. For example, T5B35D60 stands for 5%
181 (by volume) triacetin, 35% (by volume) biodiesel and 60% (by volume) diesel. That there was
182 no phase separation as the blends were tested at room temperature for 96 hours to ensure
183 miscibility and stability. It was observed that there was no phase separation. Readers can refer
184 to ref. [20] for more specific information about the fuels used in this study and their effects on
185 engine performance and exhaust emission parameters under different engine operating
186 conditions.

187 It should be noted that beside oxygen, hydrogen and carbon, fuel also contains small trace of
188 sulfur, nitrogen and metals [31]. Our main concern in this investigation was to know the fuel
189 oxygen, as it influences significantly to suppress diesel emissions. We did not account for
190 nitrogen and sulfur to cope up with 100%.

191

192

193

194 Table 3. Properties of tested fuels

Fuel	D100	T5B35D60	B100	T4B96	T8B92	T10B90	T100
O (wt%)	0	6.02	10.93	12.25	13.57	14.23	44.00
C (wt%)	85.1	80.46	76.93	75.81	74.73	74.19	49.53
H (wt%)	14.8	13.47	12.21	11.97	11.74	11.63	6.42
Density @15°C (g/cc)	0.84	0.866	0.87	0.882	0.893	0.898	1.159
HHV (MJ/kg)	44.79	41.74	39.9	39.02	38.15	37.72	18.08
LHV (MJ/kg)	41.77	38.92	37.2	36.38	35.57	35.16	16.78
KV@40°C (mm ² /s)	2.64	3.66	4.82	4.94	5.06	5.12	7.83
Stoichio- metric air (kg _a /kg _f)	14.89	13.64	12.59	12.33	12.07	11.94	6.02
Formula	C _{7.09} H _{14.8}	C _{6.71} H _{13.47} O _{0.38}	C _{6.41} H _{12.21} O _{0.68}	C _{6.32} H _{11.97} O _{0.77}	C _{6.23} H _{11.74} O _{0.85}	C _{6.18} H _{11.63} O _{0.89}	C ₅ H ₁₄ O ₆
H/C	0.17	0.167	0.159	0.158	0.157	0.156	-
O/C	0	0.0749	0.142	0.162	0.182	0.192	-
S/C	<0.1	<0.1	<0.1	<0.1	<0.1	<0.1	-

195

196 The biodiesel used in this study was provided by Eco Tech Biodiesel Pty Ltd. in Australia.

197 Table 4 shows the fuel technical specification.

198

199

200

201

202

203 Table 4. Fuel technical specification, Fuel technical specification, Eco Tech Biodiesel,
 204 SPECHECK LABORATORIES P/L, Mittagong, NSW 2575, Australia

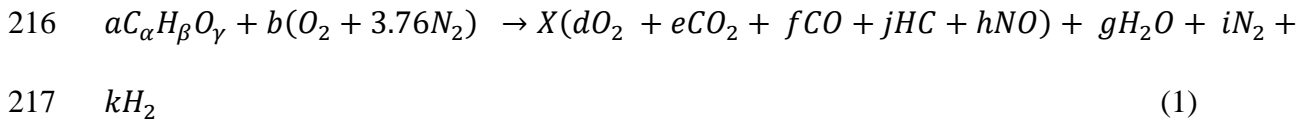
METHOD	TEST	RESULT	SPECIFICATION	UNITS
EN12662	Total contamination	11.1	24	max mg/kg
ASTM D664	Total Acid Number	0.25	0.8	max mgKOH/g
ASTM D7501	Cold soak filterability	201	360	max sec
ASTM D874	Sulphated Ash	<0.01	0.02	max %
ASTM D4350	Carbon Residue (10% res)	0.108	0.3	max %
ASTM D6584	Free glycerol	0.01	0.02	max %
EN14110	Alcohol content	0.02	0.2	max %
ASTM D93	Flash point	>130	120	min °C
ASTM D130	Copper Corrosion	1A	1	max -
ASTM D6304	Moisture content	312	500	ppm
EN14112	Oxidation stability	9.52	9	min h
EN14103	Ester content	97.4	96.5	min %
ASTM D6584	Monoglycerides	0.246	0.8	max %
ASTM D6584	Total glycerol	0.089	0.25	max %
ASTM D6371	Cold filter plugging point	-2	-	- °C
ASTM D2068	Filter blocking tendency (B100)	1.05	2	max -
ASTM D1160	Distillation temp @90% rec	316	360	max °C

205

206 2.3 Combustion analysis

207 The number of moles (n) of each individual reactant required for a chemical reaction can be
 208 obtained through the knowledge of the mass of the compound set to undergo the reaction. From
 209 the knowledge of the moles of the chemical reactant, the reaction equation can be balanced
 210 when some of the emission concentrations of individual products have been measured. In this
 211 study, the measured emission products found in the emission data include CO, O₂, CO₂, HC
 212 and NO. From these measured compounds, N₂, H₂O, and H₂ can be obtained by balancing the
 213 chemical equation. Concentrations of other substances such as nitrogen dioxide (NO₂) and

214 particulate matter (PM) were sufficiently low compared to others and were neglected in this
215 analysis. The combustion equation can be written as Equation (1):



218 where the coefficients a, b, d, e, f, g, h, i, j, k are the mole fractions of the respective components
219 and X is the number of moles of the measured products. It is assumed that no trace of water
220 vapour is contained in the intake air and the calculations assumed that the air was dried, thus
221 the air contains 21% oxygen and 79% nitrogen. The coefficients of both the reactant and
222 exhaust product are important in the energy and exergy analysis of the combustion system, as
223 it is needed to carry out further analysis [24]. The values of α , β and γ are identified from fuel
224 properties as they have been measured and presented in Table 3 for each fuel (C, O and H
225 (wt%)). Air and fuel flow rates are available from experimental data, so “a” and “b” are known.
226 Emission concentrations in exhaust are also measured experimentally and the remaining
227 coefficients has been calculated using experimental emission data and material balance from
228 the combustion equation.

229

230 2.4 Oxygen ratio

231 The equivalence ratio has been a more widely-used term to show the ratio of fuel and air to that
232 of its stoichiometric ratio. This may be misleading in the case of oxygenated fuels, which have
233 oxygen molecules in their chemical formulae. Pham et al. [32] considered the use of an
234 equivalent parameter to the equivalence ratio termed the oxygen ratio (OR). This is because
235 OR gives a more appropriate measure of stoichiometry for oxygenated fuels. OR which
236 considers the oxygen content in fuel is defined as the ratio of total atoms in the mixture to the
237 total required oxygen atoms for the stoichiometric combustion and is given by Equation (2):

238
$$OR = \frac{O_{2,fuel} + O_{2,air}}{\text{Stoichiometric oxygen requirement}} \quad (2)$$

239

240 where $O_{2,fuel}$ and $O_{2,air}$ are the masses of oxygen in the fuel and intake air ,respectively.

241 Therefore OR changes during the experiment by changing the engine load and speed as under

242 different engine operating condition, the intake air amount is different.

243 2.5 Energy analysis

244 For the energy analysis to be carried out, some simplifying assumptions are made [33]:

245 ➤ The entire engine, which excludes the dynamometer, is considered to be a control
246 volume running at steady-state.

247 ➤ The combustion air and exhaust gas each form ideal gas mixtures.

248 ➤ Changes in the potential and kinetic energy of the air, fuel and exhaust gases are
249 negligible.

250 ➤ The lower heating value (LHV) of the fuel is used due to the vapour state of water in
251 the exhaust product.

252 With the aforementioned assumptions, the fuel input energy rate (\dot{Q}_f) into the control volume
253 is given by Equation (3):

254
$$\dot{Q}_f = \dot{m}_f \cdot LHV \quad (3)$$

255 where \dot{m}_f and LHV are the mass flow rate (kg/s) and the lower heating value (kJ/kg) of the fuel
256 respectively.

257 The brake power (\dot{W}) generated by the engine can be obtained from the engine torque (T) and
258 speed (N) as shown in Equation (4):

259

260
$$\dot{W} = \frac{2\pi NT}{60} \text{ (kW)} \quad (4)$$

261 where N is in rpm and T is in kNm. The mass and energy balance for the control volume can
 262 be represented by the continuity equation and the first law of thermodynamics [33]. The mass
 263 balance which equates the mass inflow to the mass outflow is represented in Equation (5):

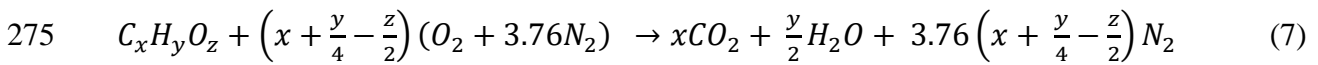
264
$$\sum m_i = \sum m_e \quad (5)$$

265 The energy balance is given in Equation (6) using the brake power from Equation (4).

266
$$\dot{Q}_{cv} - \dot{W} = h_p - h_R \quad (6)$$

267
$$h_p = \sum_p n_e (h_f^0 + \Delta \bar{h})_e, \quad h_R = \sum_R n_i (h_f^0 + \Delta \bar{h})_i$$

268 where subscripts p , R , cv , i and e represent the product, reactant, control volume, inlet and exit
 269 states, respectively. n denotes the number of moles while h_f^0 and Δh represent the standard
 270 enthalpy of formation and enthalpy change due to a change of state. Standard Tables of
 271 thermodynamic [34] properties are used to extract the standard enthalpy and the enthalpy
 272 change at the exit temperature of the gases. To obtain the enthalpy of the reactant (h_R), the
 273 formation enthalpy is determined from complete combustion of the fuel when the theoretical
 274 quantity of air is supplied [18]. This is mathematically stated as shown in Equation (7):



276 The standard enthalpy of formation for the fuel can be obtained utilising the first law of
 277 thermodynamics; the heat released from the reaction equals the lower heating value of the fuel.

278 The enthalpy of the fuel can be obtained from Equation (8):

279
$$(h_f^0)_{Fuel} = x(h_f^0)_{CO_2} + 0.5y(h_f^0)_{H_2O} + (3.76x + 0.94y - 1.88z)(h_f^0)_{N_2} + \overline{LHV} \quad (8)$$

280 The heat loss through the exhaust gases can be calculated as the difference between the energy
281 input rate from the air/fuel mixture and the control volume, which consists of the mechanical
282 work (brake power) and the heat transfer. The amount of energy brought into the system by the
283 combustion air can be ignored, as it enters the system having the same temperature as the
284 reference environment. The heat loss through the exhaust is mathematically represented as
285 shown in Equation (9):

$$286 \quad \dot{Q}_{exh} = \dot{m}_f \cdot LHV - (\dot{W} + |\dot{Q}_{cv}|) \quad (9)$$

287 To evaluate how well the engine converts heat to work, the brake thermal efficiency (BTE) is
288 introduced, and is the ratio of the brake power \dot{w} to the fuel energy input rate \dot{Q}_f , as shown in
289 Equation (10):

$$290 \quad BTE = \frac{\dot{W}}{\dot{Q}_f} \quad (10)$$

291 Another important engine characteristic is the brake specific fuel consumption (BSFC), which
292 is a measure of the amount of fuel needed to produce a kilowatt of power in one hour, and it is
293 given by Equation (11):

$$295 \quad BSFC = \frac{\dot{m}_f}{\dot{W}} 3600 \quad (11)$$

296

297 2.6 Exergy analysis

298 In order to effectively carry out the exergy analysis, assumptions used in energy analysis are
299 still valid. The reference environment in this study corresponds to an environment temperature
300 (T_0) of 298.15 K and atmospheric pressure of 1 bar. Based on this assumption, the exergy
301 balance for the control volume can be stated as Equation (12):

$$302 \quad \dot{E}_Q + \dot{E}_W = \sum \dot{m}_{in} e_{in} - \sum \dot{m}_{out} e_{out} - \dot{E}_{dest} \quad (12)$$

303 where \dot{E}_Q is the exergy flow rate accompanying the heat leaving the control volume to the
 304 environment through the cooling water; \dot{E}_W is the exergy flow accompanying work, \dot{E}_{dest} is
 305 the exergy destruction rate due to irreversibility in the control volume; also,
 306 $\sum \dot{m}_{in} e_{in}$ and $\sum \dot{m}_{out} e_{out}$ represent the rate of exergy entering and leaving the control
 307 volume. e_{in} , and e_{out} are the specific exergies of the fuel and exhaust gases, and \dot{m}_{in} and \dot{m}_{out}
 308 are the mass/molar flow rate of the fuel and exhaust gases.

309 The exergy flow rate leaving the control volume through the cooling water can be represented
 310 as shown in Equation (13):

$$311 \quad \dot{E}_Q = \sum Q_{cv} \left(1 - \frac{T_o}{T_{cw}}\right) \quad (13)$$

312 Where Q_{cv} is the heat leaving the control volume through the engine cooling water, T_o and T_{cw}
 313 are the temperatures of the reference environment and the cooling water respectively. Also, the
 314 exergy associated with the work transfer for the defined control volume is equal to the brake
 315 power. It is mathematically represented as shown in Equation (14):

$$316 \quad \dot{E}_W = \dot{W} \quad (14)$$

317

318 The input exergy rate, which is the rate of exergy entering the control volume, can be
 319 represented with the chemical exergies of the fuel and combustion air, which can be neglected
 320 due to the air entering the engine at the temperature of the reference environment. The input
 321 exergy rate can be represented as shown in Equation (15):

$$322 \quad \sum \dot{m}_{in} e_{in} = \dot{m}_f \phi |LHV| \quad (15)$$

323 where \dot{m}_f is the mass of fuel consumed, and ϕ is the chemical exergy factor of the fuel in unit
 324 mass as given in Equation (16) [35]:

$$325 \quad \phi = \left[1.0401 + 0.1728 \frac{h}{c} + 0.0432 \frac{o}{c} + 0.2169 \frac{s}{c} \left(1 - 2.0628 \frac{h}{c} \right) \right] \quad (16)$$

326 where h , c , o , and s are the mass fractions of hydrogen, carbon, oxygen and sulphur contents
 327 of the fuels from Table 3. The chemical exergy of liquid fuel, is related to its LHV by using an
 328 empirical coefficient (ϕ) calculated based on atomic compositions [36, 37].

329 The exhaust gas exergy, which is the rate of exergy leaving the control volume, can be
 330 represented by the sum of two constituents: thermomechanical (\bar{e}_{tm}) and chemical (\bar{e}_{th})
 331 exergies of the fuel. The exhaust gas exergy is represented by Kotas [35] as shown in Equations
 332 17 and 18:

$$333 \quad \sum \dot{m}_{out} e = n_f (\bar{e}_{tm} + \bar{e}_{th})$$

$$334 \quad \bar{e}_{tm} = \sum_i a_i [\bar{h}_{i,T} - \bar{h}_{i,T_0} - T_0 (\bar{s}_{i,T}^0 - \bar{s}_{i,T_0}^0)] + \bar{R} T_0 \ln \frac{p}{p_0} \quad (17)$$

$$335 \quad \bar{e}_{ch} = \bar{R} T_0 \sum_i a_i \left(\ln \frac{y_i}{y_{i,00}} \right) \quad (18)$$

336 where h and s are the specific enthalpy and absolute entropy of the exhaust gases, n is the molar
 337 flow rate, R is the general gas constant, T_0 is the temperature of the reference environment, p
 338 and p_0 are the exhaust gas pressure and reference pressure, y_i is the molar fraction of the
 339 exhaust gas component i , and $y_{i,00}$ is the molar fraction of gases in the reference environment
 340 tabulated below. The mole fractions are obtained by balancing the chemical equation of each
 341 combustion process. In addition, the exhaust gas pressure is considered to be the same as the
 342 atmospheric pressure as it is discharged to the environment, thus causing the pressure term of
 343 the thermomechanical exergy to equate to zero. Thermophysical properties of gases can be
 344 obtained from [34]. Experimental data (such as air and fuel mass flow rates, emission data etc.)

345 which varies for each operating condition is used to find the component coefficients in the
 346 combustion equation and used with exhaust temperature for each operating condition to obtain
 347 the exergy from Eq. 17 and 18.

348 Table 5: Definition of Environment [38]

Reference environment	Mole fraction
O ₂	20.35
CO	0.0007
CO ₂	0.0345
Others	0.91455
H ₂ O	3.03
N ₂	75.67
SO ₂	0.0002
H ₂	0.00005

349

350 From Equations 12-18, the irreversibility associated with the combustion process can be
 351 obtained. If the exergy balance equation is rearranged (Equation 12), the exergy destruction
 352 can be mathematically stated as:

$$353 \quad \dot{E}_{dest} = \sum \dot{m}_{in} \epsilon_{in} - \dot{E}_Q - \dot{E}_W - \sum \dot{m}_{out} \epsilon_{out} \quad (19)$$

354 The ratio of each of the exergy components to the input exergy rate is an important indication
 355 of exergy analysis, as it shows the fraction of the fuel exergy carried away through the different
 356 processes. These fractions obtained from the combustion of a particular fuel can be compared
 357 with similar fractions obtained from the combustion of a different fuel whose heating value
 358 varies from the other fuel. In order to determine the fraction of the fuel exergy converted to
 359 work, second law efficiency is considered. Second law efficiency (also known as exergetic
 360 efficiency) is the fraction of the fuel exergy converted to the desired product (work), and is
 361 mathematically stated in Equation (20):

$$362 \quad \eta_{ii} = \frac{\dot{E}_W}{\dot{E}_f} = \frac{\dot{E}_W}{\dot{m}_f e_f^{ch}} \quad (20)$$

373 3. RESULTS AND DISCUSSION

374 In this section, parameters such as brake specific fuel consumption, thermal efficiency, fuel
375 energy and heat loss, as well as the exergetic efficiency and the exergy loss accompanying the
376 exhaust gas are presented. In all figures, the six fuels are differentiated by using different
377 colours; the three engine speeds are shown with three different shapes, and four engine loads
378 are displayed with four shape sizes (the higher the load, the bigger the shape size). For the
379 exergy analysis, the exergy parameters are analysed according to engine operation parameters,
380 i.e. the exergy content of the fuel (fuel exergy) converted to work (brake power), and losses
381 through the exhaust (exhaust exergy) or destruction due to the irreversibilities (exergy
382 destruction). Relationships between energy and exergy parameters were also discussed in
383 details

374

375 3.1 Energy analysis

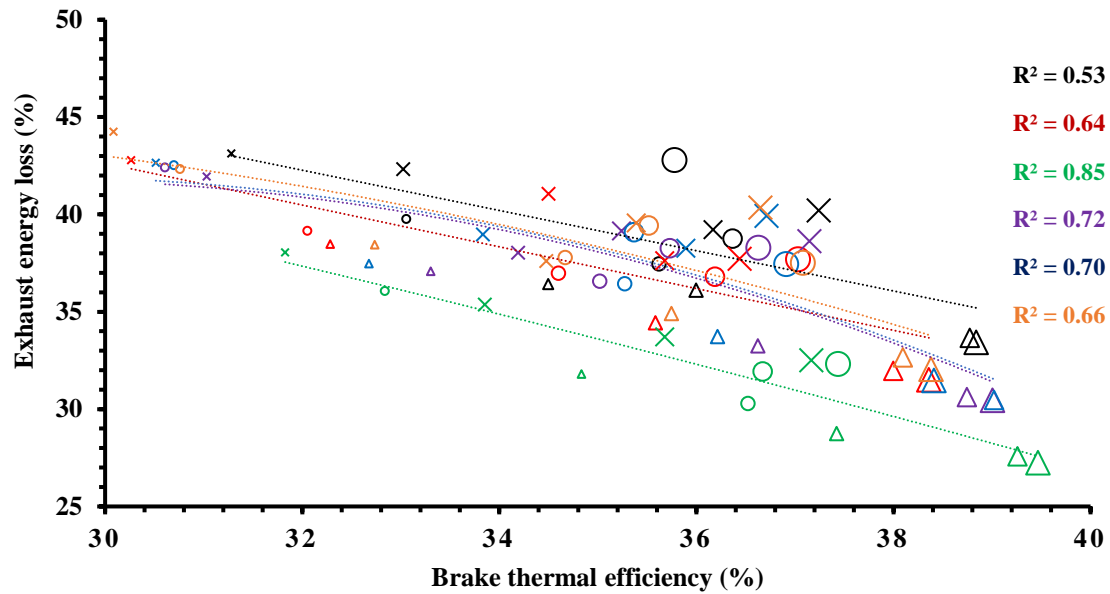
376 As the main objective of this work is to look at the exergy parameters, just two main parameters
377 of energy analysis (i.e., BTE and exhaust loss) which are more relevant to exergy analysis will
378 be presented firstly. From the experimental data, brake thermal efficiency (BTE) was obtained
379 and presented in Fig. 2. BTE is a good indicator of how well the chemical energy of the fuel is
380 transformed into useful work as it depends on the brake power, heating value and mass of fuel.
381 From Fig. 2, it is seen that with increasing load, BTE increases. In this study, by increasing the
382 speed, the BTE is seen to be decreased. Considering the variation in BTE among fuels, it is
383 seen that the BTE is higher for B100 in this study, which shows a different trend to the literature.
384 This higher thermal efficiency is a good indication that higher energy input in the form of heat
385 is converted to work. However, it will be discussed further in exergy analysis. It is seen that
386 using oxygenated fuels improves the thermal efficiency when compared with diesel fuel.
387 Improved combustion owing to better mixture formation with oxygen-rich fuels and lower

388 exhaust temperatures [39]. The lower exhaust temperature with the oxygenated fuels could be
389 due to the lower calorific value of the fuels, which leads to lower in-cylinder pressure and
390 temperature.

391 Heat loss through the exhaust discharge is one of the greatest sources of inefficiency. Exhaust
392 energy loss can be looked at as the ratio of the exhaust energy to the fuel input energy to
393 indicate the proportion of the fuel energy carried away by the exhaust gases as presented in Fig.
394 2. At low loads and high RPMs, over 40% of the fuel energy is wasted by exhaust discharge.
395 It is seen that increasing the load reduces the proportion of fuel energy carried away by the
396 exhaust gas. The decrease in the proportion of fuel energy carried out by the exhaust gas at full
397 load shows that more energy has been converted to work (causing an increase in BTE), with a
398 slight increase in heat transfer loss. Also, an increase in exhaust energy loss is observed as the
399 speed increases. Considering the fuels, it is observed that the highest proportion of fuel energy
400 wasted as the exhaust gas is for D100 at all operating modes, while B100 had the least exhaust
401 energy loss. This high/low exhaust loss causes a corresponding decrease/increase in other
402 energy forms to which the fuel energy is converted.

403 From Fig. 2, it is seen that operating the engine at low speed and high load yields higher BTE
404 and lower exhaust energy loss, with B100 having the highest BTE and lowest exhaust energy
405 loss. This indicates a better energy-to-work conversion at high load. Also, it is seen that the
406 values obtained when the engine is operated at 75% and 100% load at 1472 rpm are almost the
407 same for the exhaust loss and brake thermal efficiency showing the same order of energy
408 converted to useful work is wasted by exhaust discharge. It is worth noting that increasing the
409 speed at constant load reduces the brake thermal efficiency and heat transfer rate, with a
410 corresponding increase in the proportion of the fuel energy leaving the combustion chamber as
411 exhaust gas. This is true as the increase in speed increases the amount of fuel taken into the
412 combustion chamber, resulting in improper mixing and incomplete combustion.

413 Load% (Shape Size): 100(9) – 75(7) – 50(5) – 25 (3) ----- Speed (rpm): 1472 (Δ) 1865 (O) 2257 (x)
 414 D100(0%) T5B35D60(6.02%) B100(10.93%) T4B96(12.25%) T8B92(13.57%) T10B90(14.23%)



415 Fig. 2: Exhaust energy loss vs. brake thermal efficiency at 12 engine operating modes for the
 416 6 tested fuels
 417

418
 419 3.2 Exergy analysis

420 From the second law of thermodynamics, the fuel exergy converted to work is calculated for
 421 different fuels and engine operating conditions. Unlike fuel energy, fuel exergy does not only
 422 depend on the mass and heating value of the fuel, but also on the chemical exergy factor of the
 423 fuel (Equation 15) [19]. From Table 3, it is seen that LHV decreases with an increase in the
 424 oxygen content of the fuel, thus causing a decrease in fuel exergy among oxygenated fuels.
 425 D100, which has no oxygen content, is expected to have the highest fuel exergy at all operating
 426 modes, while T10B90, with the highest oxygen content, should present the least fuel exergy.

427 Regarding the effect of engine operating condition on exergy and energy analyses, the air-fuel
 428 and equivalence ratio can be used. However, these two parameters cannot consider the effect
 429 of fuel oxygen content when oxygenated fuels are used, especially given that the fuel oxygen

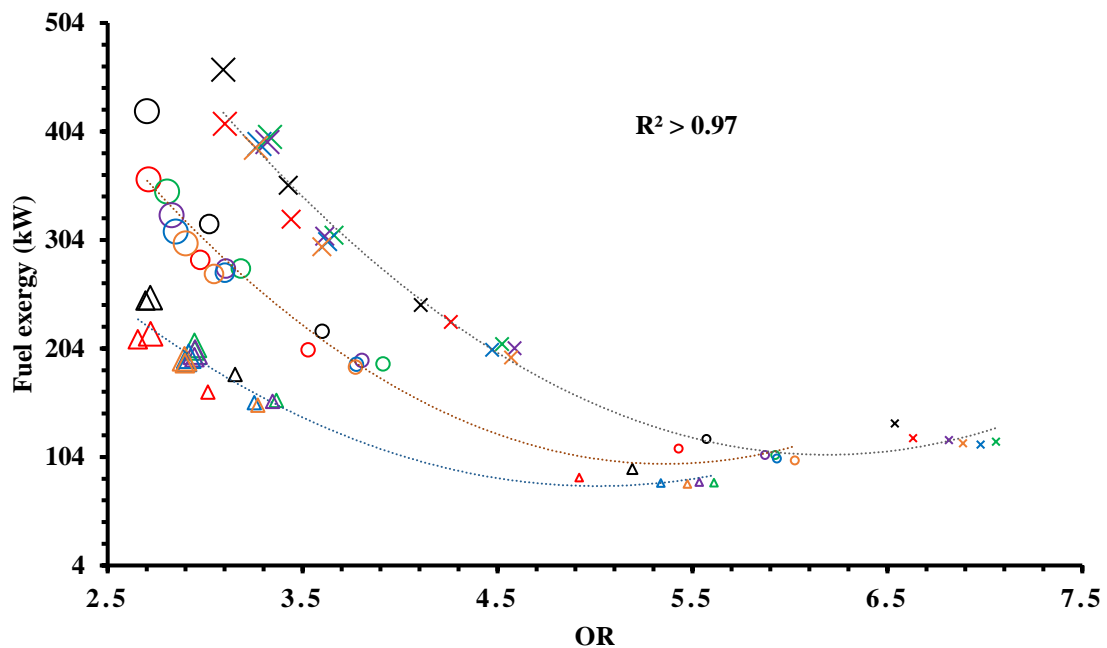
430 content has a significant effect on engine performance and emissions [20, 22-24]. Therefore, it
431 is more representative to consider the OR in this work [20].

432 From Fig. 3, it is seen that the OR decreases by increasing the engine load. It is also shown that
433 increasing the engine speed is associated with an increased OR. As can be seen in Fig. 3., at
434 three different engine speeds, there is a strong correlation between fuel exergy and OR, which
435 confirms the strong correlation between fuel exergy and engine load. Increase in load and speed
436 cause an increase in the mass of injected fuel, which increases the fuel exergy. This increase in
437 fuel exergy causes a corresponding increase in the ways by which energy is converted into
438 various forms. Also, from Fig. 3, it is seen that at a specific load and speed, an increase in fuel
439 oxygen content decreases the fuel exergy. This is due to the reduction in LHV of fuels by
440 increasing the oxygen content as discussed before.

441

442 Load% (Shape Size): 100(9) – 75(7) – 50(5) – 25 (3) ----- Speed (rpm): 1472 (Δ) 1865 (O) 2257 (x)

443 D100(0%) T5B35D60(6.02%) B100(10.93%) T4B96(12.25%) T8B92(13.57%) T10B90(14.23%)



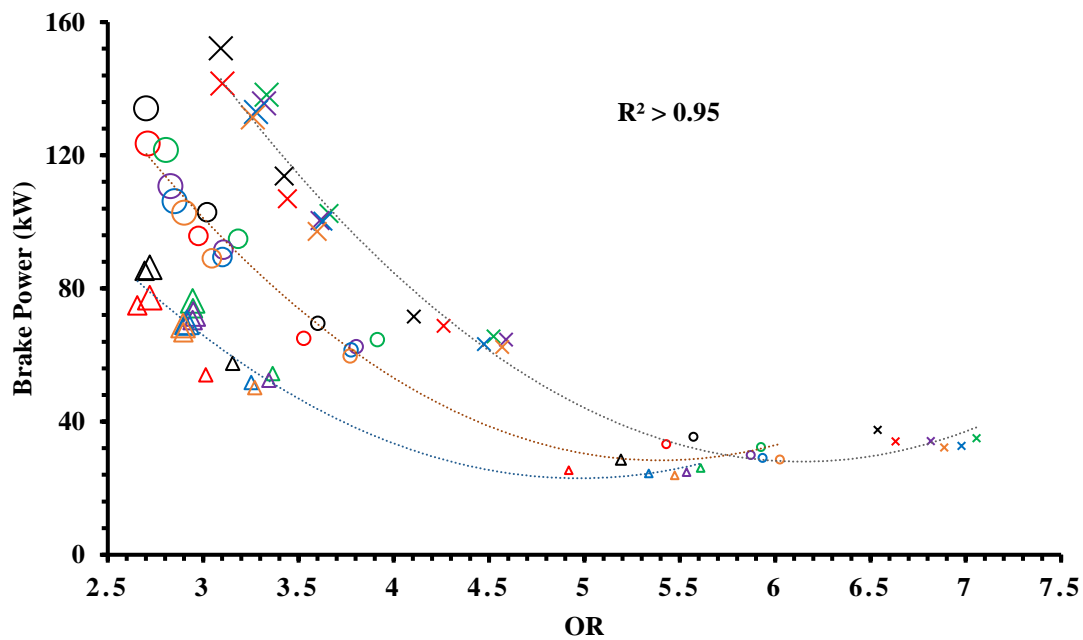
444

445 Fig. 3. Fuel Exergy vs. OR at 12 engine operating modes for the 6 tested fuels

446

447 Brake power is the parameter to present the exergy of the useful work produced by the engine
 448 at different speeds and loads for the various fuels is shown in Fig. 4. It is seen that D100 has
 449 the highest brake power compared to the oxygenated fuels used at all operating conditions. For
 450 the oxygenated fuels, it is seen that the power produced decreases with an increase in oxygen
 451 content and is largely attributed to the low heating value of oxygenated fuels. This decrease in
 452 heating value of the fuel owing to the increase in oxygen content also significantly influences
 453 the fuel energy as shown before. Increasing either the speed or the load causes a corresponding
 454 increase in the power produced as more fuel is injected into the chamber, thus increasing the
 455 energy input rate.

456
 457 **Load% (Shape Size): 100(9) – 75(7) – 50(5) – 25 (3) ----- Speed (rpm): 1472 (Δ) 1865 (O) 2257 (x)**
 458 **D100(0%) T5B35D60(6.02%) B100(10.93%) T4B96(12.25%) T8B92(13.57%) T10B90(14.23%)**



459
 460 Fig. 4. Brake power vs. OR at 12 engine operating modes for the 6 tested fuels

461
 462 With a fraction of the fuel exergy converted to the brake power, the remaining is lost in varying
 463 proportions through the exhaust gas or cooling water losses, or destroyed as a consequence of

464 a number of irreversible processes, such as mixing, combustion and friction. Considering the
465 fuel exergy lost through the exhaust, Fig. 5 shows the variation of the exhaust exergy loss with
466 OR at different speeds and loads. The effect of increase in speed at a constant load on exhaust
467 exergy loss can clearly be observed in this figure. With the increase in speed, the exhaust
468 exergy loss increases as the time available for complete combustion decreases [40]. This
469 increase in exhaust exergy loss leads to a corresponding decrease in all other fuel exergy values.

470 As the exhaust temperature is the key indication of the exergy loss, a plot of the exhaust exergy
471 against the exhaust temperature is presented in Fig. 6. The fraction of the fuel exergy lost
472 through the exhaust for the different fuels used is seen to follow similar trendlines, as shown
473 in Fig. 6. However, B100 followed a different path and it is represented by a separate trendline.
474 These trendlines, which are polynomials of order 2, have a very high regression of above 0.99
475 for all speeds. The exhaust exergy loss decreases by decreasing the exhaust gas temperature as
476 shown in this figure. It is seen that increasing the load increases the temperature of the exhaust
477 gas as expected. From the analysis carried out, it is seen that diesel fuel has the highest exhaust
478 exergy loss owing to its high exhaust temperature, at all operating modes [41]. Lower exhaust
479 temperature and exergy loss are seen with oxygenated fuels due to their lower heating values.
480 This indicates a decrease in combustion temperature which has a positive effect on the exhaust
481 exergy loss as it occurs in the lean flame zone [42].

482

483

484

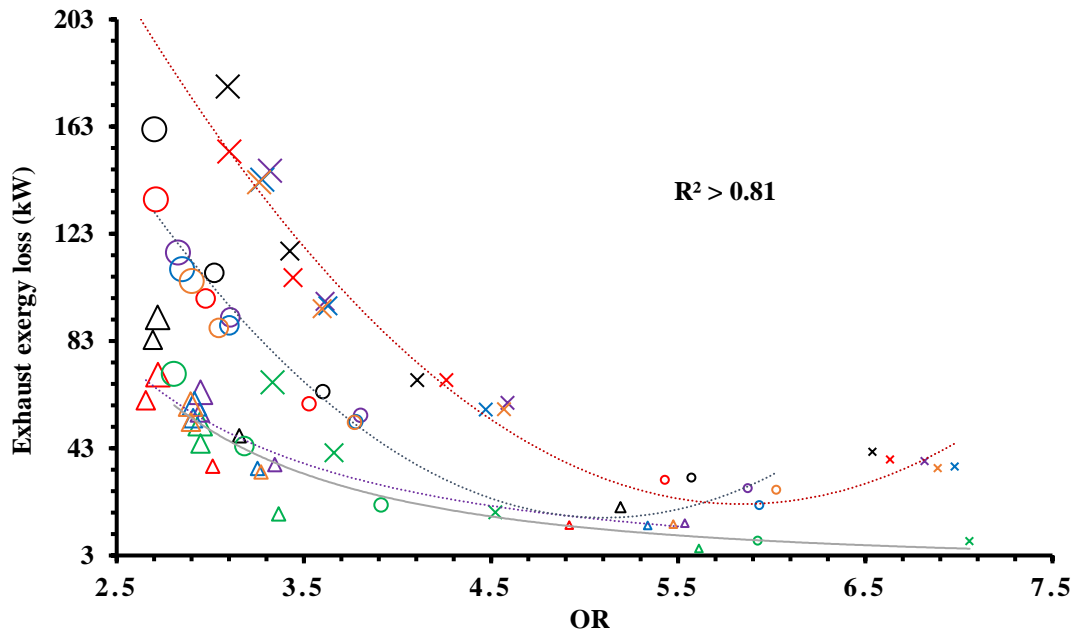
485

486

487

488 Load% (Shape Size): 100(9) – 75(7) – 50(5) – 25 (3) ----- Speed (rpm): 1472 (Δ) 1865 (O) 2257 (x)

489 D100(0%) T5B35D60(6.02%) B100(10.93%) T4B96(12.25%) T8B92(13.57%) T10B90(14.23%)



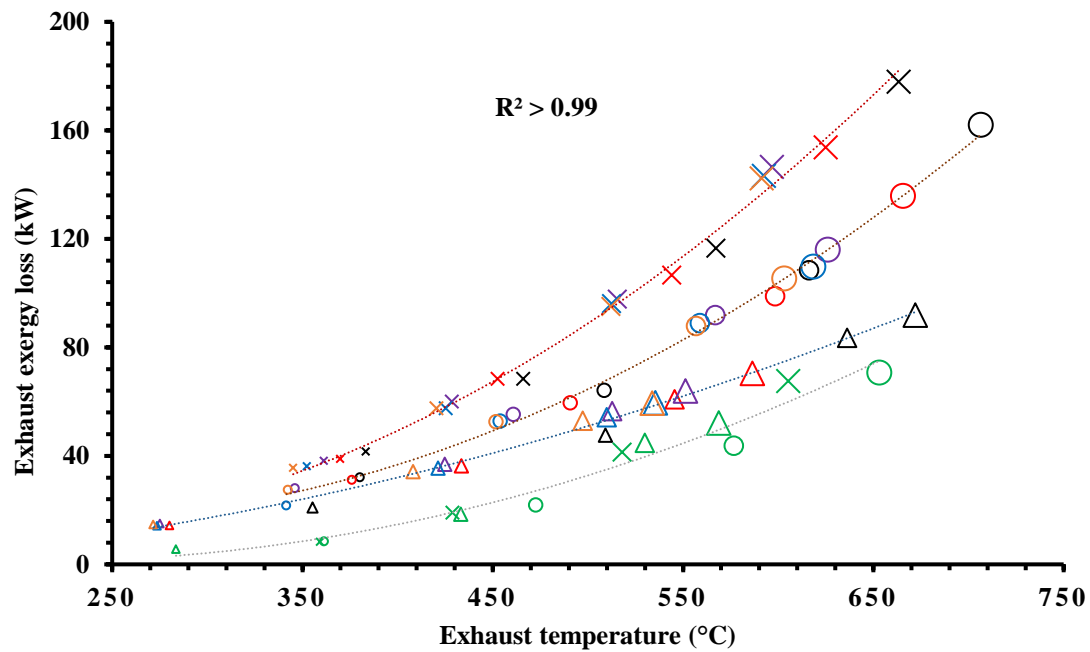
490

491 Fig.5: Exhaust exergy loss vs. OR at 12 engine operating modes for the 6 tested fuels

492

493 Load% (Shape Size): 100(9) – 75(7) – 50(5) – 25 (3) ----- Speed (rpm): 1472 (Δ) 1865 (O) 2257 (x)

494 D100(0%) T5B35D60(6.02%) B100(10.93%) T4B96(12.25%) T8B92(13.57%) T10B90(14.23%)

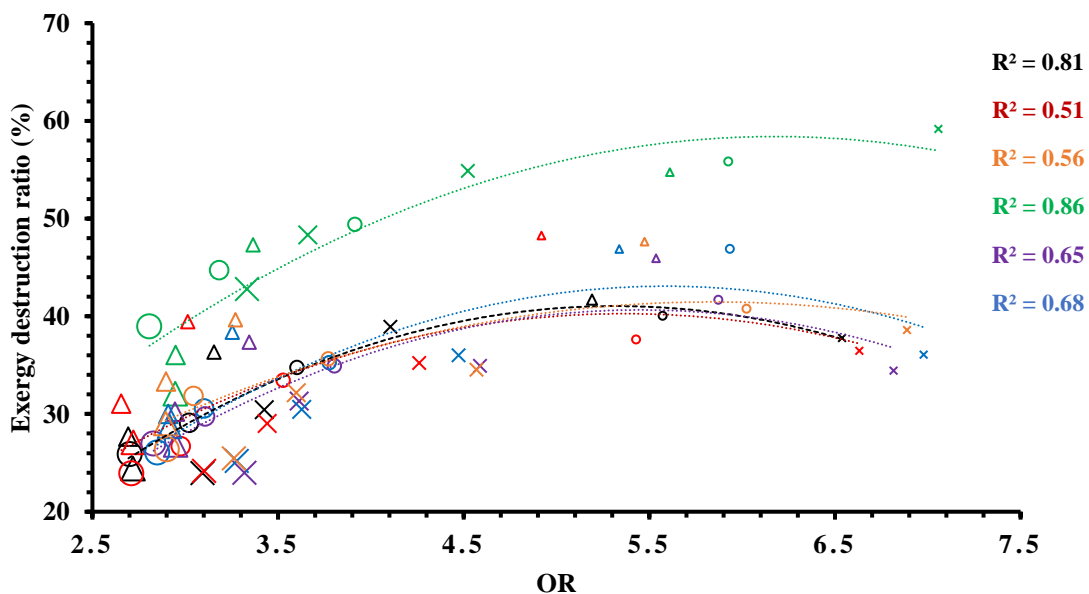


495

496 Fig.6. Exhaust exergy loss vs. exhaust gas temperature at 12 engine operating modes for the 6
497 tested fuels

498 Factors such as combustion, turbulence, flow losses and mixing are sources of irreversibility
 499 and are accounted for as exergy destruction. Since fuel exergy varies with different fuels,
 500 exergy destruction ratio, which represents the proportion of fuel exergy destroyed during the
 501 combustion, would be an important parameter for comparing different fuels in this study. From
 502 Fig. 7, it is seen that the exergy destruction is lower at high loads showing the combustion is
 503 happening in condition closer to the ideal with less destruction of exergy. As can be seen,
 504 exergy destruction decreases with an increase in both engine load and speed in general.
 505 Considering the fuels at all modes, it is seen that the variation in exergy destruction is higher
 506 at low loads between the fuels while in high loads all fuels (except B100) are performing more
 507 similar. D100 has the lowest destruction ratio and B100 shows the highest destruction ratio at
 508 all modes. It is seen that at full load, the lowest destruction is achieved with D100 yielding a
 509 destruction ratio of 23.9%, occurring at the highest speed, but with a corresponding high
 510 exhaust exergy loss of 38.6%, owing to its high temperature.

511 **Load% (Shape Size): 100(9) – 75(7) – 50(5) – 25 (3) ----- Speed (rpm): 1472 (Δ) 1865 (O) 2257 (x)**
 512 **D100(0%) T5B35D60(6.02%) B100(10.93%) T4B96(12.25%) T8B92(13.57%) T10B90(14.23%)**



513 Fig.7. Exergy destruction ratio vs. OR at 12 engine operating modes for the 6 tested fuels
 514

515

516 As exergy loss and destruction are sometimes interpreted similarly by mistake, they are
517 presented separately in Fig. 8. This figure shows the variation of exergy destruction and the
518 exhaust exergy loss for different fuels at different engine operating modes. A reverse trend
519 between exhaust exergy loss and exergy destruction is found from this figure showing that the
520 parameters affecting exergy destruction are affecting the exergy loss in opposite way. D100
521 maintaining the highest exhaust exergy loss at all operating modes. This is largely attributed to
522 high exhaust gas temperature for diesel as shown before. This is contrary to B100, as the
523 proportion of fuel exergy lost through the exhaust is seen to be the lowest in all operating modes
524 and exergy destruction is the highest. B100 showed a very high destruction and on the other
525 hand a low exergy loss, thus shifting slightly from the path taken by other fuels tested. This
526 fuel exhibits the highest cetane number (lowest ignition delay) meaning the lowest level of
527 premixed combustion with this fuel which leads to more incomplete combustion condition and
528 more exergy destruction. Exergy destruction ratio is seen to be increased with an increase in
529 engine speed with significant reduction in exhaust exergy loss. Also, with load increase, the
530 proportion of the fuel exergy destroyed reduces and a corresponding increase in the exhaust
531 exergy loss is observed. This increase in exhaust exergy loss at increasing load (and also speed)
532 is caused mainly by the increase in temperature at which the gases leave the combustion
533 chamber.

534

535

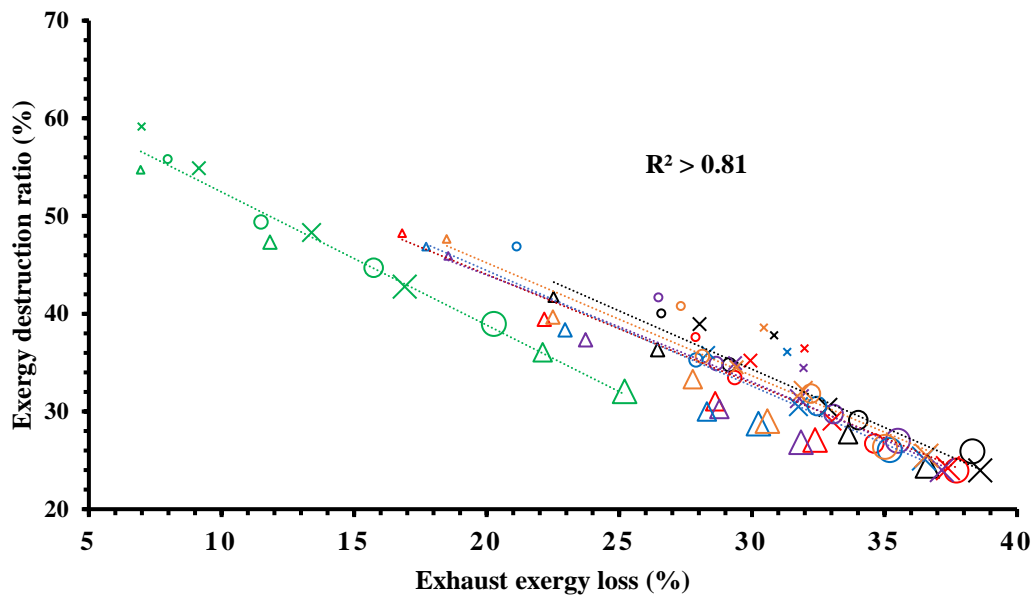
536

537

538

539

540 Load% (Shape Size): 100(9) – 75(7) – 50(5) – 25 (3) ----- Speed (rpm): 1472 (Δ) 1865 (O) 2257 (x)
 541 D100(0%) T5B35D60(6.02%) B100(10.93%) T4B96(12.25%) T8B92(13.57%) T10B90(14.23%)



542
 543 Fig. 8. Exergy destruction ratio vs. Exhaust exergy loss at 12 engine operating modes for the
 544 6 tested fuels

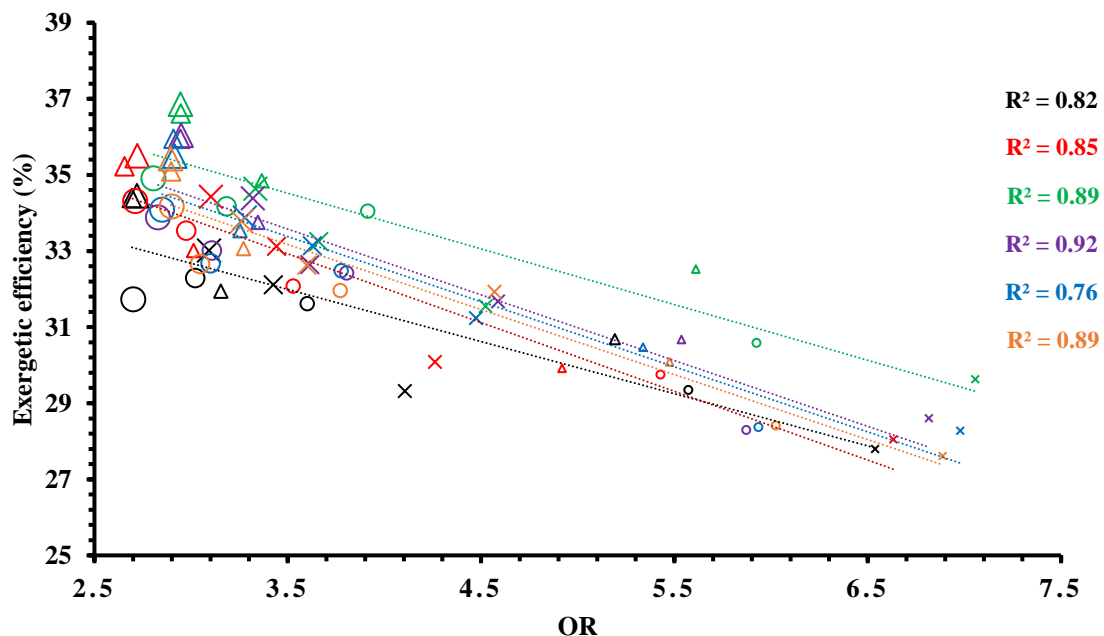
545
 546 Fig. 9 shows the exergetic efficiency, which defined as the ratio of brake power to the fuel
 547 exergy, for different conditions. The proportion of extracted useful work is seen to be increased
 548 with an increase in load and the maximum values happen at the lowest speed and 100% load
 549 for all the fuels. This is similar to its energy counterpart, but has a lower efficiency, whose
 550 percentage difference with the BTE ranges from 6.56% for D100 and increases with an increase
 551 in oxygen content to 7.02% in T10B90. The exergetic efficiency gives a better idea of engine
 552 operation as it takes into account both the first and second laws of thermodynamics as well as
 553 the exergy destructions and exergy losses. At a constant load, the exergetic efficiency is seen
 554 to be decreased by increasing speed causing the minimum exergetic efficiency to be seen at
 555 25% load operated at 2257 rpm. This is attributed to the decrease in volumetric efficiency of
 556 the combustion chamber as less time is required to fill the cylinder [43].

557 The other important finding is the exergetic efficiency improvement with the use of oxygenated
 558 fuels, with the exception at 25% load. This increase in exergetic efficiency is primarily due to
 559 the better combustion of these oxygenated fuels and less losses, compared to D100. The highest
 560 exergetic efficiency is exhibited by B100 at all operating modes, and thus can be considered a
 561 better quality fuel than other fuels used, if we assume the exergetic efficiency as the measure
 562 of fuel quality. At low loads, the lower exergetic efficiency was observed by some of the
 563 oxygenated fuels (T4B96, T8B92 and T10B90) when compared with D100. It could be
 564 attributed to low in-cylinder pressure and also low combustion temperature, as an increase in
 565 load provides an appropriate condition for combustion for this fuels [43]. This is seen to be
 566 reversed with an increase in load, as higher combustion temperatures with the oxygenated fuels
 567 were obtained, thus converting more heat into useful work.

568

569 **Load% (Shape Size): 100(9) – 75(7) – 50(5) – 25 (3) ----- Speed (rpm): 1472 (Δ) 1865 (O) 2257 (x)**

570 **D100(0%) T5B35D60(6.02%) B100(10.93%) T4B96(12.25%) T8B92(13.57%) T10B90(14.23%)**



571

572 Fig. 9. Exergetic efficiency at 12 engine operating modes for the 6 tested fuels

573

574 3.3 Exergy and fuel consumption relationships

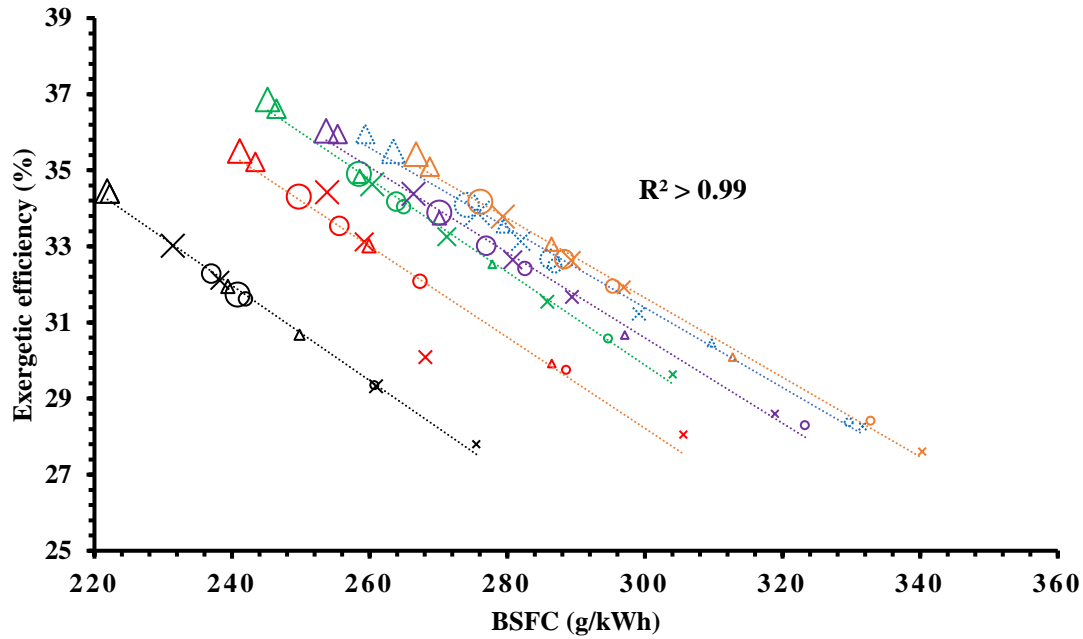
575 The correlation between exergetic efficiency and BSFC for fuels at different speeds and loads
576 shows a linear trend and is presented in Fig. 10. Considering the BSFC, it is seen that at all
577 three speeds, by increasing the engine load the BSFC reduces and the minimum BSFC was
578 obtained at full load. Also, at any given load, an increase in speed causes an increase in BSFC.
579 As can be seen, the BSFC increases with an increase in oxygen content. This is because an
580 increase in the oxygen content of the fuel causes a decrease in the lower heating value [44].
581 The oxygen content of the fuel is a good indicator of the loss of heating value and increased
582 fuel consumption [39]. It is seen that D100 had the lowest BSFC at all modes, owing to its high
583 heating value. The minimum BSFC was 0.22 g/kWh at full load and 1475 rpm belongs to D100,
584 while the maximum BSFC was observed at 0.342 g/kWh with the higher oxygenated fuel
585 (T10B90) operating at 25% load and 2257 rpm.

586 Considering BSFC against exergetic efficiency, maximum exergetic efficiency can deliver the
587 lowest BSFC. Values of BSFC decrease with decreasing speed and increasing load, causing a
588 corresponding increase in the exergetic efficiency and operating the engine at low speed (1472
589 rpm) and high load yields the lowest possible BSFC and the highest exergetic efficiency for
590 each individual fuel considered. It is seen that D100 has the lowest BSFC and exergetic
591 efficiency, while B100 shows the highest exergetic efficiency with moderate BSFC. As can be
592 seen, maximum exergetic efficiency is for B100 and addition of triacetin to biodiesel (which
593 results in a lower heating value) increases the BSFC and decreases the exergetic efficiency [20].
594 From the plot the increase in diesel content of the oxygenated fuel, causes a decrease in BSFC,
595 as observed for T5B35D60.

596

597

598 Load% (Shape Size): 100(9) – 75(7) – 50(5) – 25 (3) ----- Speed (rpm): 1472 (Δ) 1865 (O) 2257 (x)
 599 D100(0%) T5B35D60(6.02%) B100(10.93%) T4B96(12.25%) T8B92(13.57%) T10B90(14.23%)



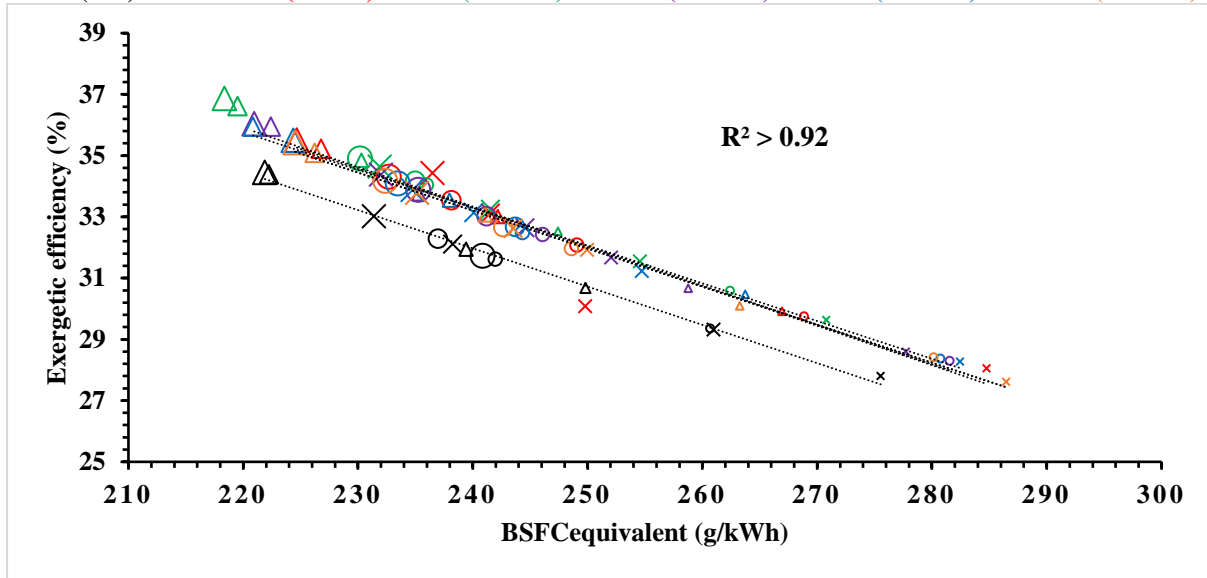
600
 601 Fig.10. Exergetic Efficiency vs. BSFC at 12 engine operating modes for the 6 tested fuels

602
 603 As the LHV is different for the fuels used in this study, $BSFC_{equivalent}$ is calculated to develop
 604 a further analysis of the results presented in Fig. 11. Equivalent brake specific fuel consumption
 605 $BSFC_{equivalent}$ represents the amount of diesel fuel equivalent for producing the same amount
 606 of power and it is defined as follow [45]:

$$607 \quad BSFC_{equivalent} = BSFC \times LHV_{blend} / LHV_{diesel} \quad (21)$$

608 The results of exergetic efficiency vs. $BSFC_{equivalent}$ are presented in Figure 11. All the
 609 biofuels are following almost the same trendlines, however, the trend is still similar to Figure
 610 10. As can be seen, improving the exergetic efficiency means achieving lower $BSFC_{equivalent}$
 611 for each fuel as presented on this figure. Among all the tested fuels, the $BSFC_{equivalent}$ for
 612 B100 is the lowest at different operating conditions making it a better alternative fuel. At low
 613 load and high speed, the $BSFC_{equivalent}$ of all the tested fuels are higher than diesel (except
 614 for B100). This trend changes by increasing the load and speed for different fuels.

615 Load% (Shape Size): 100(9) – 75(7) – 50(5) – 25 (3) ----- Speed (rpm): 1472 (Δ) 1865 (O) 2257 (x)
 616 D100(0%) T5B35D60(6.02%) B100(10.93%) T4B96(12.25%) T8B92(13.57%) T10B90(14.23%)



617

618 Fig.11. Exergetic Efficiency vs. BSFCequivalent at 12 engine operating modes for the 6
 619 tested fuels

620

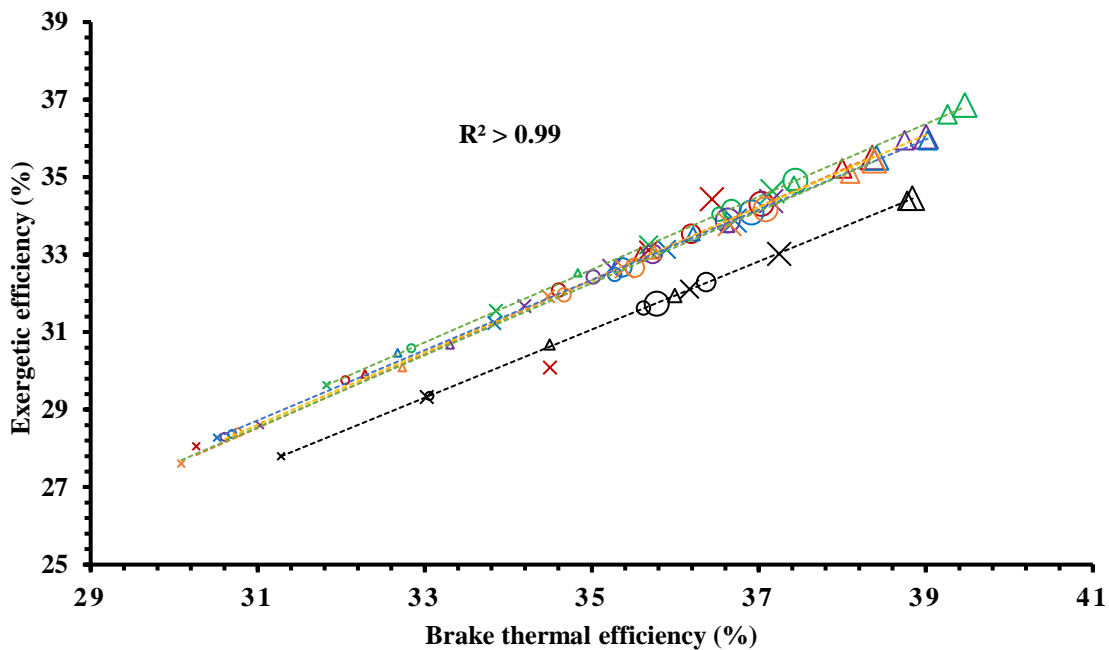
621 A linear trend can be obtained when the BTE is plotted against the exergetic efficiency in Fig.
 622 12. This is because the BTE and exergetic efficiency are both used to measure the quantity of
 623 the heat converted to work with respect to first and second law analysis. Comparing the
 624 exergetic efficiency against BTE, it is seen that the BTE is higher for all operating conditions
 625 than the exergetic efficiency owing to the lower value of energy input rate when compared to
 626 the high chemical exergy of the fuel used in the exergy analysis. Also, the exergetic efficiency
 627 combines both first and second law efficiency to account for the usefulness of the energy being
 628 supplied.

629 From both efficiencies, it is seen that they depend on the lower heating value of the fuel. The
 630 lower heating value of D100 is seen to be the highest, and decreases with an increase in fuel
 631 oxygen content while T10B90 has the lowest heating value. From Fig. 12, it is seen that D100
 632 clearly distinguishes itself from the other fuels owing to the low fuel consumption and high
 633 heating value (minimum difference with the oxygenated fuels used in this study is

634 approximately 4800 kJ/kg). This high heating value of D100, which produces less power with
 635 respect to the energy input, causes a visible decrease in the exergetic efficiency of the diesel
 636 fuel as it moves below the other fuels' line. It is also seen that the oxygenated fuels are closely
 637 packed and increase linearly. This cluster is mainly attributed to the closeness of their
 638 respective heating value and fuel consumption. With respect to oxygenated fuels, it is seen that
 639 T10B90 (with the lowest heating value) had the lowest BTE and exergetic efficiency.

640

641 Load% (Shape Size): 100(9) – 75(7) – 50(5) – 25 (3) ----- Speed (rpm): 1472 (Δ) 1865 (O) 2257 (x)
 642 D100(0%) T5B35D60(6.02%) B100(10.93%) T4B96(12.25%) T8B92(13.57%) T10B90(14.23%)



643

644 Fig. 12: Exergetic Efficiency vs. Brake thermal efficiency at 12 engine operating modes for
 645 the 6 tested fuels

646

647 4. Conclusion

648 This investigation used the first and second laws of thermodynamics to analyse the influence
 649 of oxygenated fuels on the quality and quantity of energy in a diesel engine using diesel, waste
 650 cooking biodiesel, and a highly oxygenated additive, triacetin. The six fuels used in this study

651 had a range of fuel oxygen content from 0 to 14 wt%. The experimental engine performance
652 and emission data were collected at 12 different engine operating modes (three different speeds
653 and four engine loads), and were used to calculate and analyse the energy and exergy
654 parameters, such as: fuel energy, thermal efficiency, exhaust energy loss, exergetic efficiency,
655 destruction efficiency and exhaust exergy. The following conclusions were obtained from this
656 study:

- 657 • Since the investigated fuels were oxygenated, this study used the oxygen ratio (OR)
658 instead of the equivalence ratio.
- 659 • OR increased with decreasing engine load and increasing engine speed.
- 660 • OR showed strong correlations (with a high R^2) for different energy and exergy
661 parameters.
- 662 • Increasing the OR decreased the fuel exergy, exhaust exergy, destruction efficiency and
663 exergetic efficiency, while it increased the exergy destruction.
- 664 • Strong correlations with high R^2 was found between exhaust energy loss and brake
665 thermal efficiency, exhaust exergy and exhaust temperature, destruction efficiency and
666 exhaust efficiency, exergetic efficiency and brake specific fuel consumption, exergetic
667 efficiency and thermal efficiency.
- 668 • Using oxygenated fuels resulted in higher brake thermal efficiency, OR, exergy
669 destruction and exergetic efficiency; and lower exhaust energy loss, fuel exergy, engine
670 power, exhaust exergy, exhaust temperature and brake specific fuel consumption.
- 671 • Increased in oxygen content resulted in better combustion, as irreversibilities were seen
672 to be reduced with the addition of triacetin, but with a corresponding loss in heating
673 value.
- 674 • Lower exhaust temperature obtained with oxygenated fuels resulted in lower exhaust
675 exergy losses and higher exergetic efficiency.

676 **Acknowledgement**

677 The authors would like to thank Professor Zoran Ristovski, Dr Mostafizur Rahman, Dr Farhad
678 Hossein and Mr. Noel Hartnett from QUT and Mr Andrew Elder from DynoLog Dynamometer
679 Pty Ltd. for their help in this research.

680

681 **References**

- 682 [1] R.E. Ebel, M.P. Croissant, J.R. Masih, K.E. Calder, R.G. Thomas. International energy
683 outlook: US Department of Energy. Washington Quarterly. 19 (1996) 70-99.
- 684 [2] A. Demirbaş. Biodiesel fuels from vegetable oils via catalytic and non-catalytic
685 supercritical alcohol transesterifications and other methods: a survey. Energy conversion and
686 Management. 44 (2003) 2093-109.
- 687 [3] K. Cheikh, A. Sary, L. Khaled, L. Abdelkrim, T. Mohand. Experimental assessment of
688 performance and emissions maps for biodiesel fueled compression ignition engine. Applied
689 Energy. 161 (2016) 320-9.
- 690 [4] M. Rahman, A. Pourkhesalian, M. Jahirul, S. Stevanovic, P. Pham, H. Wang, et al. Particle
691 emissions from biodiesels with different physical properties and chemical composition. Fuel.
692 134 (2014) 201-8.
- 693 [5] H. Omidvarborna, A. Kumar, D.-S. Kim. A laboratory investigation on the effects of
694 unsaturated bonds and chain lengths of different biodiesel feedstocks on carbon dioxide, carbon
695 monoxide, and methane emissions under low-temperature combustion. Journal of
696 Environmental Chemical Engineering. 4 (2016) 4769-75.
- 697 [6] A. Manikandan. Application of Exergy (Availability) Analysis to Spark-Ignition Engines
698 Operation Considering a Single-Zone Combustion Model. Proceedings of National Conf on
699 Recent Innovations in Science Engineering & Technology, Pune, 2014.
- 700 [7] M.A. Rosen. Exergy concept and its application. Electrical Power Conference, 2007 EPC
701 2007 IEEE Canada. IEEE2007. pp. 473-8.
- 702 [8] Y. Li, M. Jia, Y. Chang, S.L. Kokjohn, R.D. Reitz. Thermodynamic energy and exergy
703 analysis of three different engine combustion regimes. Applied Energy. 180 (2016) 849-58.
- 704 [9] M. Chahartaghi, M. Sheykhi. Energy and exergy analyses of beta-type Stirling engine at
705 different working conditions. Energy Conversion and Management. 169 (2018) 279-90.
- 706 [10] J.A. Caton. The thermodynamic characteristics of high efficiency, internal-combustion
707 engines. Energy Conversion and Management. 58 (2012) 84-93.
- 708 [11] M. Nabi, M. Rasul. Influence of second generation biodiesel on engine performance,
709 emissions, energy and exergy parameters. Energy Conversion and Management. 169 (2018)
710 326-33.
- 711 [12] E.J. Cavalcanti, M. Carvalho, A.A. Ochoa. Exergoeconomic and exergoenvironmental
712 comparison of diesel-biodiesel blends in a direct injection engine at variable loads. Energy
713 Conversion and Management. 183 (2019) 450-61.
- 714 [13] H. Feng, X. Wang, J. Zhang. Study on the effects of intake conditions on the exergy
715 destruction of low temperature combustion engine for a toluene reference fuel. Energy
716 Conversion and Management. 188 (2019) 241-9.

- 717 [14] A. Karthikeyan, J. Jayaprabakar. Energy and exergy analysis of compression ignition
718 engine fuelled with rice bran biodiesel blends. *International Journal of Ambient Energy*. 40
719 (2019) 381-7.
- 720 [15] C. Rakopoulos, E. Giakoumis. Simulation and exergy analysis of transient diesel-engine
721 operation. *Energy*. 22 (1997) 875-85.
- 722 [16] E. Hürdoğan. Thermodynamic analysis of a diesel engine fueled with diesel and peanut
723 biodiesel. *Environmental Progress & Sustainable Energy*. 35 (2016) 891-7.
- 724 [17] S. Jafarmadar, P. Nematı. Exergy analysis of diesel/biodiesel combustion in a homogenous
725 charge compression ignition (HCCI) engine using three-dimensional model. *Renewable*
726 *Energy*. 99 (2016) 514-23.
- 727 [18] F. Meisami, H. Ajam. Energy, exergy and economic analysis of a Diesel engine fueled
728 with castor oil biodiesel. *International Journal of Engine Research*. 16 (2015) 691-702.
- 729 [19] B. Sayın Kul, A. Kahraman. Energy and Exergy Analyses of a Diesel Engine Fuelled with
730 Biodiesel-Diesel Blends Containing 5% Bioethanol. *Entropy*. 18 (2016) 387.
- 731 [20] A. Zare, M.N. Nabi, T.A. Bodisco, F.M. Hossain, M.M. Rahman, Z.D. Ristovski, et al.
732 The effect of triacetin as a fuel additive to waste cooking biodiesel on engine performance and
733 exhaust emissions. *Fuel*. 182 (2016) 640-9.
- 734 [21] A. Zare, T.A. Bodisco, M.N. Nabi, F.M. Hossain, M. Rahman, Z.D. Ristovski, et al. The
735 influence of oxygenated fuels on transient and steady-state engine emissions. *Energy*. 121
736 (2017) 841-53.
- 737 [22] M.N. Nabi, A. Zare, F.M. Hossain, M.M. Rahman, T.A. Bodisco, Z.D. Ristovski, et al.
738 Influence of fuel-borne oxygen on European Stationary Cycle: Diesel engine performance and
739 emissions with a special emphasis on particulate and NO emissions. *Energy conversion and*
740 *management*. 127 (2016) 187-98.
- 741 [23] H. Song, K.S. Quinton, Z. Peng, H. Zhao, N. Ladommatos. Effects of oxygen content of
742 fuels on combustion and emissions of diesel engines. *Energies*. 9 (2016) 28.
- 743 [24] J. Jena, R.D. Misra. Effect of fuel oxygen on the energetic and exergetic efficiency of a
744 compression ignition engine fuelled separately with palm and karanja biodiesels. *Energy*. 68
745 (2014) 411-9.
- 746 [25] M. Nour, A.M. Attia, S.A. Nada. Combustion, performance and emission analysis of
747 diesel engine fuelled by higher alcohols (butanol, octanol and heptanol)/diesel blends. *Energy*
748 *Conversion and Management*. 185 (2019) 313-29.
- 749 [26] Z. Han, B. Li, W. Tian, Q. Xia, S. Leng. Influence of coupling action of oxygenated fuel
750 and gas circuit oxygen on hydrocarbons formation in diesel engine. *Energy*. 173 (2019) 196-
751 206.
- 752 [27] H. Sayyaadi, M. Babaie, M.R. Farmani. Implementing of the multi-objective particle
753 swarm optimizer and fuzzy decision-maker in exergetic, exergoeconomic and environmental
754 optimization of a benchmark cogeneration system. *Energy*. 36 (2011) 4777-89.
- 755 [28] H. Sayyaadi, M. Baghsheikhi, M. Babaie. Improvement of energy systems using the soft
756 computing techniques. *International Journal of Exergy*. 19 (2016) 315-51.
- 757 [29] A. Zare, T.A. Bodisco, M.N. Nabi, F.M. Hossain, Z.D. Ristovski, R.J. Brown. Engine
758 performance during transient and steady-state operation with oxygenated fuels. *Energy & fuels*.
759 31 (2017) 7510-22.
- 760 [30] A. Zare, M.N. Nabi, T.A. Bodisco, F.M. Hossain, M. Rahman, T.C. Van, et al. Diesel
761 engine emissions with oxygenated fuels: A comparative study into cold-start and hot-start
762 operation. *Journal of cleaner production*. 162 (2017) 997-1008.
- 763 [31] S. van Dyk, J. Su, J.D. Mcmillan, J. Saddler. Potential synergies of drop-in biofuel
764 production with further co-processing at oil refineries. *Biofuels, Bioproducts and Biorefining*.
765 13 (2019) 760-75.

- 766 [32] P.X. Pham, T.A. Bodisco, Z.D. Ristovski, R.J. Brown, A.R. Masri. The influence of fatty
767 acid methyl ester profiles on inter-cycle variability in a heavy duty compression ignition engine.
768 Fuel. 116 (2014) 140-50.
- 769 [33] C. Sayin, M. Hosoz, M. Canakci, I. Kilicaslan. Energy and exergy analyses of a gasoline
770 engine. International Journal of Energy Research. 31 (2007) 259-73.
- 771 [34] R.E. Sonntag, C. Borgnakke, G.J. Van Wylen, S. Van Wyk. Fundamentals of
772 thermodynamics. Wiley New York 2003.
- 773 [35] T. Kotas. The Exergy Method of Thermal Plant Analysis. Reprint Edition. Krieger
774 Malabar, Florida, 1995.
- 775 [36] S. Fateh. Bi-directional Solid Oxide Cells used as SOFC for Aircraft APU system and as
776 SOEC to produce fuel at the airport. (2016).
- 777 [37] E. Querol, B. Gonzalez-Regueral, J.L. Perez-Benedito. Practical approach to exergy and
778 thermoeconomic analyses of industrial processes. Springer Science & Business Media 2012.
- 779 [38] M.J. Moran, H.N. Shapiro, D.D. Boettner, M.B. Bailey. Fundamentals of engineering
780 thermodynamics. John Wiley & Sons 2010.
- 781 [39] P. Sekmen, Z. Yılbaşı. Application of energy and exergy analyses to a CI engine using
782 biodiesel fuel. Mathematical and Computational Applications. 16 (2011) 797-808.
- 783 [40] M. Ghazikhani, M. Hatami, B. Safari, D.D. Ganji. Experimental investigation of exhaust
784 temperature and delivery ratio effect on emissions and performance of a gasoline–ethanol two-
785 stroke engine. Case Studies in Thermal Engineering. 2 (2014) 82-90.
- 786 [41] X. Liu, R. Bansal. Thermal Power Plants: Modeling, Control, and Efficiency Improvement.
787 CRC Press 2016.
- 788 [42] Y.H. Tan, M.O. Abdullah, C. Nolasco-Hipolito, N.S.A. Zauzi, G.W. Abdullah. Engine
789 performance and emissions characteristics of a diesel engine fueled with diesel-biodiesel-
790 bioethanol emulsions. Energy Conversion and Management. 132 (2017) 54-64.
- 791 [43] G. Khoobbakht, A. Akram, M. Karimi, G. Najafi. Exergy and energy analysis of
792 combustion of blended levels of biodiesel, ethanol and diesel fuel in a DI diesel engine. Applied
793 Thermal Engineering. 99 (2016) 720-9.
- 794 [44] A. Fayyazbakhsh, V. Pirouzfard. Comprehensive overview on diesel additives to reduce
795 emissions, enhance fuel properties and improve engine performance. Renewable and
796 Sustainable Energy Reviews. 74 (2017) 891-901.
- 797 [45] G. Chen, Y. Shen, Q. Zhang, M. Yao, Z. Zheng, H. Liu. Experimental study on combustion
798 and emission characteristics of a diesel engine fueled with 2, 5-dimethylfuran–diesel, n-
799 butanol–diesel and gasoline–diesel blends. Energy. 54 (2013) 333-42.